Bond densities and electronic structure of amorphous SiN_x:H

M. M. Guraya, H. Ascolani, and G. Zampieri
Centro Atómico Bariloche, Comisión Nacional de Energía Atómica (CNEA), 8400 San Carlos de Bariloche, Río Negro, Argentina

J. I. Cisneros, J. H. Dias da Silva, and M. P. Cantão
Instituto de Fisica, Universidade Estadual de Campinas (UNICAMP), Caixa Postal 6165, 13 081 Campinas, São Paulo, Brazil
(Received 1 March 1990)

We present a study of amorphous hydrogenated silicon-nitrogen alloys (a-SiN_x:H, $0 \le x < 1.5$) prepared by the rf reactive sputtering method. By combining results of x-ray photoemission spectroscopy, electron-energy-loss spectroscopy, and optical absorption, all the atom and bond densities and the kind and mean number of nearest neighbors of Si and N atoms are determined. For $x < 1$, Si—N bonds increase at the expense of Si—Si bonds; N atoms are almost fully coordinated by three Si atoms, whereas Si atoms have N, H, and other Si atoms as nearest neighbors. For $x > 1$, Si—N bonds increase at the expense of both Si—Si and Si—H bonds; however, this is not enough to saturate the three N valencies with Si and some N—H and possibly N—N bonds begin to appear. The opening of the optical gap occurs at $x \cong 1.1$ when the ratio of the densities of Si—Si bonds to Si—N bonds has fallen below 0.10. Near stoichiometry, substantial amounts of Si—Si and N—H bonds are observed. The possibility of segregation into pure silicon and stoichiometric silicon nitride is discussed by analyzing the Si $2p$ line shape. A linear relationship between the Si $2p$ chemical shift and the mean number of N-atom nearest neighbors of Si is observed; a charge transfer of $0.35e$ per Si—N bond is determined.

I. INTRODUCTION

Silicon nitride is a material widely used in the ceramic and microelectronic industries. This has prompted a number of studies conducted to obtain silicon nitride by different methods and to determine its structural and electrical properties. It is mostly prepared as thin amorphous films which, in general, are nonstoichiometric and contain H in concentrations between 10 at. % and 40 at. %.

Aiyama *et al.*[1] and Misawa *et al.*[2] have studied the amorphous structure of near-stoichiometric compounds by x-ray and neutron diffraction, finding that the short-range order strongly resembles that of the crystalline forms. The electronic structure of a-SiN_x, in the range $0 \le x < 2$, has been the subject of a very complete investigation performed by Kärcher *et al.*[3] using x-ray photoelectron spectroscopy (XPS). They thoroughly analyzed the valence bands and obtained some information about the Si—N bonding by deconvoluting the Si $2p$ peak. Densities of electron states of the crystalline and amorphous forms have been calculated by Ren and Ching,[4] Robertson,[5] Ferreira and Gonçalves da Silva,[6] and Martín-Moreno *et al.*;[7] the results show that the electronic structure is completely determined by the short-range order. Defect and impurity states have been analyzed by Robertson and by Martín-Moreno *et al.*; the latter studied the properties of nonstoichiometric materials in the range $0 \le x < 2$.

We present here an analysis of some structural and electronic properties of a-SiN_x:H using different spectroscopies. Combining results of optical absorption, electron-energy-loss spectroscopy (EELS), and quantitative XPS, we determine all the atom and bond densities in the range $0 \le x < 1.5$. We also analyze the (XPS) peak shifts and line shapes to obtain more information about the bonding, especially charge transfers and distribution of Si-($Si_{4-k}N_k$) units. The preparation of the films and the optical measurements have been described previously.[8]

II. EXPERIMENTAL DETAILS

The samples were prepared on different substrates by reactive rf sputtering method. The total pressure of the gaseous mixture, Ar + N_2+H_2, was fixed at 1.5 Pa. The hydrogen flux, the substrate temperature, and the nominal rf power were kept also constant at 11 sscm, 180 °C, and 200 W, respectively. The N_2 partial pressure was varied from sample to sample in order to get the desired compositions. The ir spectra were taken with a JASCO 202 ir spectrophotometer. The optical gap was determined from the transmission in the absorption edge and nearby regions using a DMR-21 Zeiss spectrophotometer. More details about the optical measurements and sample preparation can be found in Ref. 8.

The XPS and EELS measurements were performed in an ultrahigh-vacuum (UHV) chamber with a base pressure of 10^{-10} Torr. We used a hemispherical electrostatic analyzer operated at a constant resolution of 1 eV.

For the XPS measurements we used Al $K\alpha$ radiation ($h\nu = 1486.6$ eV) from a standard Mg-Al x-ray gun. Since some samples showed evidence of charging effects, we adopted the procedure of referencing all the energies to that of photoelectrons from the Ar $2p_{3/2}$ level.[9] With this procedure, we avoid not only the energy shifts due to

charging effects, but also those due to shifts of the Fermi level in the band gap. This is an important prerequisite for the analysis of charge transfers. The price we are paying is precisely the loss of the information on the shifts of the Fermi level in the band gap.

We determined the ratio of N atoms to Si atoms from the intensity ratio of the N 1*s* and Si 2*p* photoelectron peaks. The method was calibrated by measuring the intensity ratio in crystalline α-Si_3N_4. We obtained $I(\text{N } 1s)/I(\text{Si } 2p)=2.4$, which gives a calibration constant of 0.55.

For the EELS measurements we bombarded the samples with 1-keV electrons and recorded energy-loss spectra in the derivative mode using standard modulation techniques.

Auger spectra of the samples as introduced into the UHV chamber showed contamination with O and C. After a mild ion sputtering the O concentration decreased to less than 5 at. % and C was undetectable by XPS.[10] Since the relative intensities of the N and Si signals did not change during the cleaning, we think that preferential sputtering of N is not relevant in our experiments. We will return to this point in Sec. III, when we compare our results with those of other workers.

III. RESULTS

In Table I we present the results of the optical measurements relevant to this work.[11] The optical gap E_g was obtained from the Tauc plot[12]

$$h\nu\sqrt{\epsilon_2}=\gamma(h\nu-E_g)\ , \tag{1}$$

where $h\nu$ is the photon energy and ϵ_2 is the imaginary part of the dielectric constant. Figure 1 shows E_g as a function of the N concentration x. The opening of the gap occurs before the stoichiometric concentration, in agreement with previous measurements[13] and calculations of ϵ_2.[7]

The integrated absorptions in the ir region, $I_{\text{Si—H}}$, $I_{\text{N—H}}$, and $I_{\text{Si—N}}$, correspond to the Si—H and N—H stretching and Si—N asymmetric-stretching modes, respectively. According to Brodsky *et al.*,[14] the integrated absorption of any vibrational band, I_{m-l}, can be related to the corresponding bond density:

$$N_{m\text{-}l}=A_{m\text{-}l}I_{m\text{-}l}\ , \tag{2}$$

where $N_{m\text{-}l}$ is the density of bonds formed by atoms m and l and $A_{m\text{-}l}$ is a constant. The last two rows of Table I contain the densities of bonds Si—H and N—H estimated with our integrated absorptions and the constants $A_{\text{Si—H}}=1.4\times10^{20}$ cm^{-2} and $A_{\text{N—H}}=2.8\times10^{20}$ cm^{-2}, valid for *a*-Si:H (Ref. 15) and stoichiometric silicon nitride,[16] respectively, modified for the intermediate compositions by means of the local-field correction.[14] Summing the bond densities $N_{\text{Si-H}}$ and $N_{\text{N-H}}$, we obtain the density of H atoms.

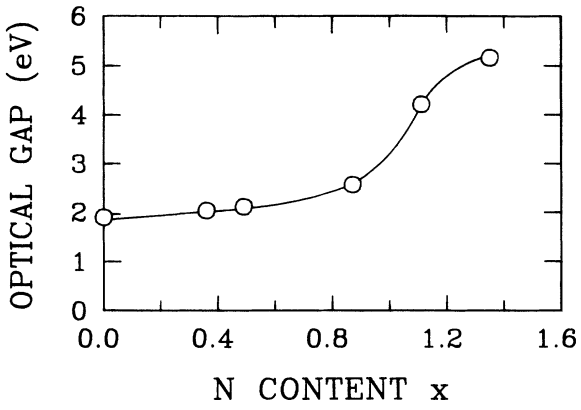

FIG. 1. Optical gap E_g as a function of the N content x.

In Table II we present the main results of the EELS and XPS measurements.

Si 2*p* and N 1*s* photoelectron spectra representative of all the samples studied are presented in Figs. 2 and 3. As discussed in Sec. II, the energies are referred to the Ar $2p_{3/2}$ level, to which we have assigned, arbitrarily, a binding energy of 242.0 eV. To characterize the line shapes, we use two parameters: the full width at half maximum, W, and an asymmetry factor defined as follows:

$$A=100\frac{\Delta_H-\Delta_L}{\Delta_H+\Delta_L}\ , \tag{3}$$

where Δ_H and Δ_L are the half-width at half maximum towards the high- and the low-binding-energy sides of the peak, respectively. In order to gain accuracy and uniformity in the determination of W and A, we have fitted the experimental line shapes with a superposition of up to five Gaussians whose intensities, positions, and widths were optimized by a least-squares method. The line shape of the Si 2*p* peak varies strongly as the N content is

TABLE I. Results of the optical measurements.

Sample no.	E_g (eV)	$I_{\text{Si—H}}$ (cm^{-1})	$I_{\text{N—H}}$ (cm^{-1})	$I_{\text{Si—N}}$ (cm^{-1})	$N_{\text{Si-H}}$ (10^{22} cm^{-3})	$N_{\text{N-H}}$ (10^{22} cm^{-3})
1	1.89	84	0	0	1.2	0
2	2.03	190	2	2276	2.3	0.06
3	2.11	201	5	3760	2.4	0.2
4	2.56	200	11	6370	2.2	0.3
5	4.21					
6	5.16	63	68	7380	0.7	1.9

TABLE II. Results of the EELS and XPS measurements.

Sample no.	x	$\hbar\omega_p$ (eV)	Si 2p E_B[a] (eV)	Si 2p W (eV)	Si 2p A (%)	N 1s E_B[a] (eV)	N 1s W (eV)	N 1s A (%)
1	0.00	17.14	99.2	1.85	+4.3			
2	0.36	19.02	99.6	2.80	+9.8	397.2	1.95	+1.5
3	0.49	19.60	100.2	3.00	+2.7	397.5	2.00	0.
4	0.87	20.57	101.3	3.00	−13.9	397.5	2.15	+1.4
5	1.11		101.4	2.45	−3.2	397.6	2.15	+1.2
6	1.35	21.90	101.9	2.40	−1.7	398.0	2.15	+1.2

[a]To determine the binding energies, we have assigned, arbitrarily, an energy of 242.0 eV to the Ar $2p_{3/2}$ level.

increased. The peak first broadens asymmetrically towards high binding energies, then towards low binding energies, and finally narrows and becomes rather symmetric again. A significant shift of the maximum from 99.2 to 101.9 eV is observed. In contrast, the N 1s peak remains practically unchanged; only a small broadening and a shift towards high binding energies are observed.

The line shape of the Si 2p peak can be used to analyze the possibility of segregation of nonstoichiometric films into amorphous silicon and stoichiometric silicon nitride.[17] In Fig. 4 we compare a synthetic spectrum produced to simulate the case of segregation with the measured Si 2p spectrum. To simulate the mixture of a-Si:H and a-Si_3N_4:H with $x=0.87$, we have combined in the right proportions the Si 2p spectra of a-Si:H and of the most nitrogenated sample ($x=1.35$). It is clear that the spectrum expected in the case of segregation is quite different from the one actually measured. Since none of our Si 2p spectra present a secondary peak or even a shoulder, we rule out the possibility of any segregation in our films.

Energy-loss spectra in the derivative mode are presented in Fig. 5. The plasmon energy increases smoothly from 17.14 eV in a-Si:H to 21.9 eV in the sample with the highest N content. In the spectrum of a-Si:H, two secondary losses, corresponding to the excitation of a surface plasmon and of two bulk plasmons, are clearly observed at 12 and 34 eV. When N is incorporated the structure of the plasmon loss broadens and no feature corresponding to surface plasmons is observable.

The important point of the possible preferential sputtering of N can now be analyzed by comparing our results with those of other workers. The Si 2p line shape is well suited for this purpose because of its variations. Our spectra are very similar to those reported by Kärcher *et al.*[3] obtained with samples prepared *in situ*,

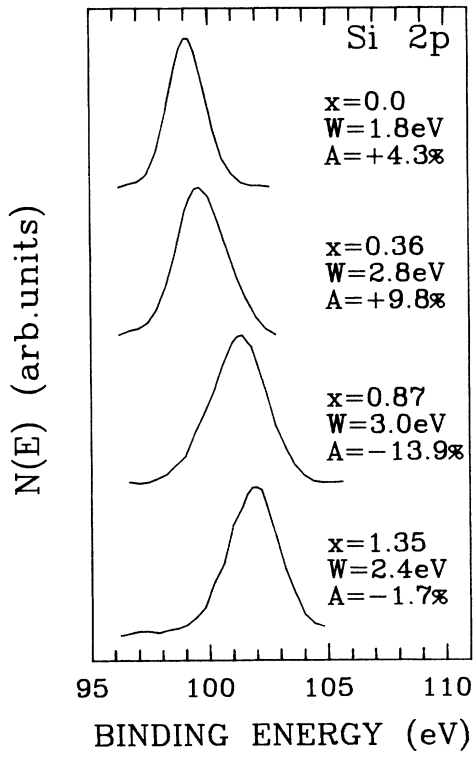

FIG. 2. Si 2p photoelectron spectra. The N content x, the peak width W, and the asymmetry factor A for each spectrum are indicated. The binding energies are referred to the Ar $2p_{3/2}$ level (see text).

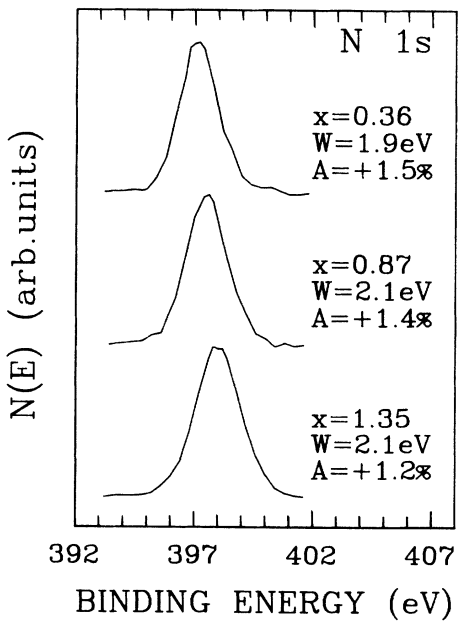

FIG. 3. N 1s photoelectron spectra.

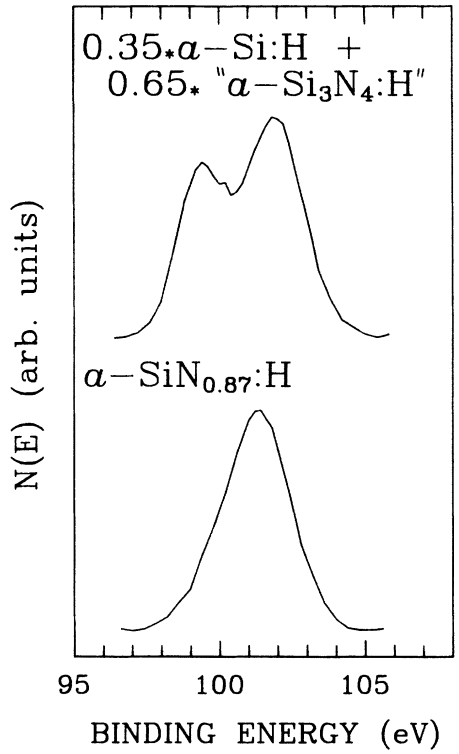

FIG. 4. Comparison of a synthetic Si $2p$ spectrum created to simulate the result in case of segregation and the actually measured Si $2p$ spectrum.

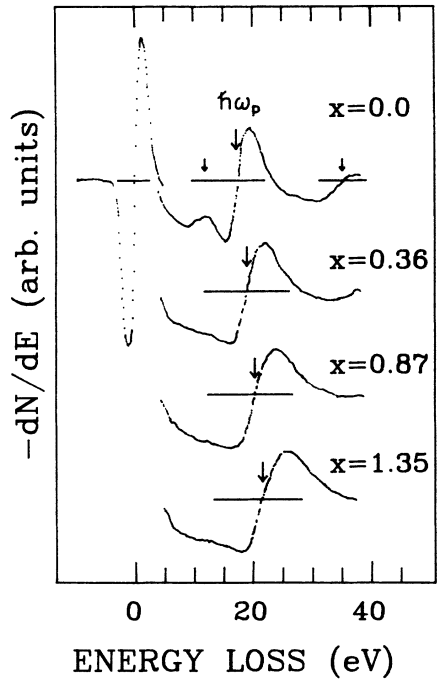

FIG. 5. Energy-loss spectra of samples with different N contents. The arrow indicates the volume-plasmon loss. The small arrows in the spectrum of a-Si:H indicate losses due to the excitation of a surface plasmon, at 12 eV, and of two volume plasmons, at 34 eV.

and, what is more important, the changes in line shape occur at similar N contents. The same result is obtained by comparing the plasmon energies. Our data of optical gap and Si-N ir absorption versus N content are also in agreement with those of Kurata *et al.*[13] and Morimoto *et al.*,[16] respectively. Thus we conclude that the mild ion sputtering used to clean the samples prior to the XPS and EELS experiments did not alter the original compositions.

IV. DISCUSSION

A. Plasmons

In the free-electron approximation the plasmon energy $\hbar\omega_p$ and the density of valence electrons, N_v, are related by

$$(\hbar\omega_p)^2=\frac{4\pi\hbar^2e^2}{m}N_v\ , \tag{4}$$

where m and e are the mass and the electric charge of the electron. This formula, derived for free-electron-like metals, has been applied successfully to many semiconductors and insulators.[18] The density of valence electrons is related to the atomic densities $N_{\rm Si}$, $N_{\rm N}$, and $N_{\rm H}$ through

$$N_v=n_{\rm Si}N_{\rm Si}+n_{\rm N}N_{\rm N}+N_{\rm H}\ , \tag{5}$$

where $n_{\rm Si}$ and $n_{\rm N}$ are the number of valence electrons per Si and N atoms.

Since $N_{\rm H}$ and the ratio $N_{\rm N}/N_{\rm Si}$ can be determined from the ir data and the XPS measurements, respectively, Eqs. (4) and (5) allow us to evaluate $N_{\rm Si}$ and $N_{\rm N}$, and finally the mass density, through

$$\rho=m_{\rm Si}N_{\rm Si}+m_{\rm N}N_{\rm N}+m_{\rm H}N_{\rm H}\ , \tag{6}$$

where $m_{\rm Si}$, $m_{\rm N}$, and $m_{\rm H}$ are the masses of Si, N, and H atoms.

In crystalline Si we measured $\hbar\omega_p=16.89$ eV. Applying Eqs. (4)–(6), we obtain $\rho=2.4$ g/cm^3 and $N_{\rm Si}=5.17\times10^{22}$ cm^{-3}, only slightly larger than the correct values $\rho=2.33$ g/cm^3 and $N_{\rm Si}=5.0\times10^{22}$ cm^{-3}.

For a-Si:H we obtain $\rho=2.35$ g/cm^3 and $N_{\rm Si}=5.0\times10^{22}$ cm^{-3}. Since this density of Si atoms in a-Si:H is only 3.3% smaller than that obtained for crystalline Si, we must assume that the plasmons penetrate only slightly into the voids of the amorphous network, and that the densities derived with Eqs (4)–(6) correspond mainly to the dense regions of the amorphous films.[19]

Before using Eqs. (4)–(6) to determine the densities of the films containing N, we must decide whether the N $2s$ electrons should be considered within the electron density n_v or not. In Fig. 6 we present the valence-band spectra of a-Si:H and of two samples with different N contents.[20] Calculated densities of states[4–7] and photoemission spectra[3] agree in that N $2s$ electrons do not mix with the other N and Si valence electrons and form the peak at $\sim$20 eV from ε_F. In spite of this corelike character of N $2s$ electrons, they are too near to the valence band to exclude *a priori* their participation in the plasma oscillation. We have therefore evaluated the mass density of

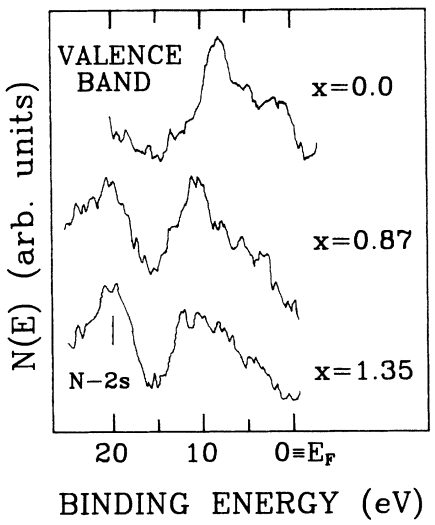

FIG. 6. Valence-band spectra excited with Al K_α radiation. The peak at 20 eV corresponds to N 2*s* electrons.

the films considering three and five electrons per N atom. The results are shown in Fig. 7. The assumption $n_N=5$ yields a nearly constant mass density. With $n_N=3$ the mass density increases with x and reaches, for the most nitrogenated sample, a density very near that of the crystalline forms of Si_3N_4:[21] 3.19 g/cm^3. Thus we conclude that the results derived with the assumption $n_N=3$ are good estimates of the mass densities of the films studied.

B. Si—N bonding

We have seen in the preceding subsection how the atomic densities N_{Si}, N_N, and N_H can be determined from the measurements of the plasmon energy, the relative concentrations of N and Si, and the densities of Si—H and N—H bonds. We will use these values to determine the densities of the main bonds: Si—Si and Si—N. A detailed balance of the total numbers of atoms and bonds gives the relations

$$3N_N = N_{Si\text{-}N} + N_{N\text{-}H} + 2N_{N\text{-}N} + N_{N\text{-}} \ , \tag{7}$$

$$4N_{Si} = N_{Si\text{-}N} + N_{Si\text{-}H} + 2N_{Si\text{-}Si} + N_{Si\text{-}} \ , \tag{8}$$

where $N_{N\text{-}}$ and $N_{Si\text{-}}$ are the densities of N and Si dangling bonds. We will neglect in the following these densities, since, according to Refs. 16 and 22, they are smaller than 10^{19} cm^{-3}, while the order of magnitude of N_{Si}, N_N, $N_{Si\text{-}H}$, and $N_{N\text{-}H}$ is 10^{22} cm^{-3}. At low N contents the density of N—N bonds can also be neglected, and Eq. (7) be used to determine the $N_{Si\text{-}N}$ term. The resulting densities of Si—N bonds (for the films with $x<1$) are shown in Fig. 8 plotted against the integrated absorptions $I_{Si\text{—}N}$; a linear relationship is observed in agreement with Eq. (2). From the slope of the line in Fig. 8, we obtain $A_{Si\text{—}N}=1.76\times10^{19}$ cm^{-2}. There is a remarkable disagreement among the published values of this constant,[16,23] probably due to structural differences in the materials used. The density of N—N bonds in the most nitrogenated sample may not be negligible. We can obtain $N_{Si\text{-}N}$ using Eq. (2) and the constant $A_{Si\text{—}N}$ just determined, and then evaluate $N_{N\text{-}N}$ with the help of Eq. (7). The resulting density is $N_{N\text{-}N}=0.64\times10^{22}$ cm^{-3}, which means that ~24% of the N atoms are bound to another N. However, since this density is a small difference between two big numbers, it may be in considerable error and should be considered only as the order of magnitude of $N_{N\text{-}N}$. The possible occurrence of this type of bond in the most nitrogenated sample will be considered again in the next subsection, when we analyze the N 1*s* peak.

Having determined the density of Si—N bonds for all the samples, we can proceed to evaluate the density of Si—Si bonds using Eq. (8).

Figure 9 shows all the atom and bond densities as a function of the N content. It is seen that the increase of the density of N atoms is accompanied by a small decrease of the density of Si atoms; the density of H atoms doubles with the incorporation of N.

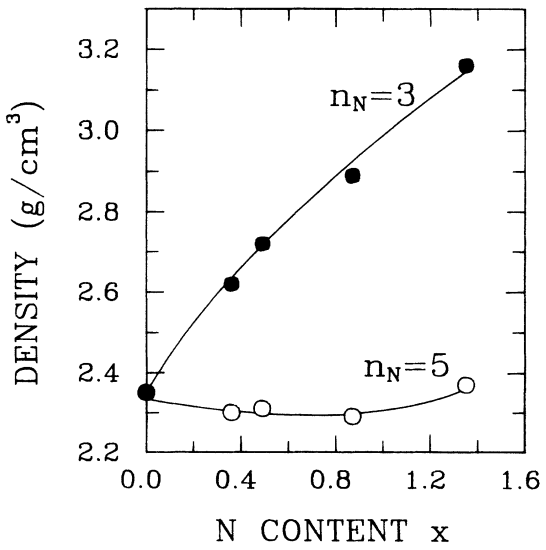

FIG. 7. Densities of the films derived from the plasmon energies assuming three and five electrons per N atom.

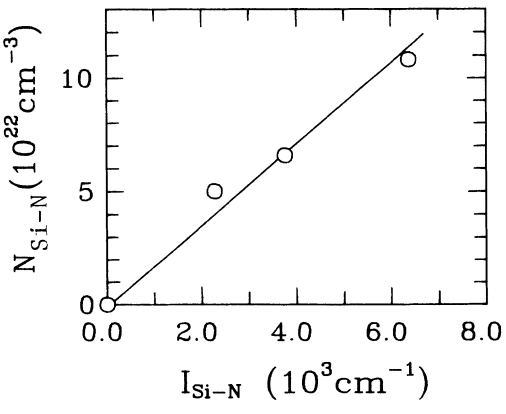

FIG. 8. Density of Si—N bonds in the films with $x<1$, plotted against the ir absorption corresponding to the Si—N asymmetric-stretching mode.

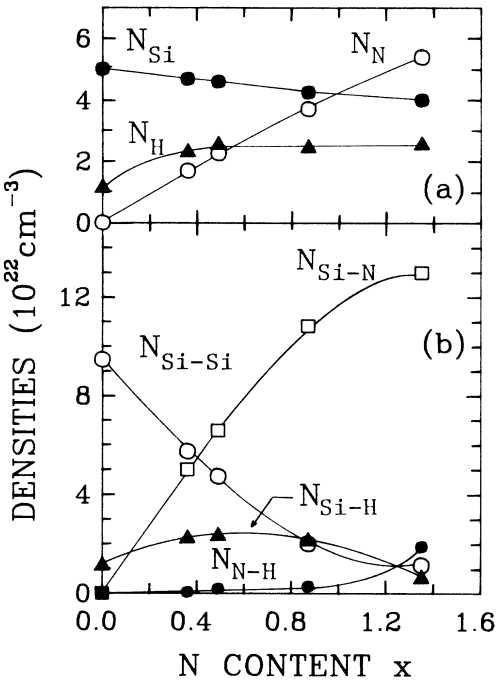

FIG. 9. Atom and bond densities as a function of the N content x.

At low N concentrations the only important change in the bond densities is the continuous replacement of Si—Si bonds by Si—N bonds. It is observed that N and H bind almost exclusively to Si atoms; the densities of N—H and N—N bonds are negligible. For N concentrations beyond $x \sim 1$ the rate of increase of $N_{Si\text{-}N}$ is smaller. Although N displaces H from the Si—H bonds, its ideal threefold coordination with Si is not reached, and some N—H and, possibly, N—N bonds appear to compensate.

According to calculations of ϵ_2 by Martín-Moreno *et al.*,[7] the optical gap is determined by transitions from states located on Si—Si bonds to the lowest states of the conduction band; the opening of the gap occurs when the density of Si—Si bonds falls below a critical value. With a simple model, considering only Si—Si and Si—N bonds for $x < 1.33$ and Si—N and N—N bonds for $x > 1.33$, they reproduce the behavior of the optical gap shown in Fig. 1 reasonably well. However, they locate the opening of the gap at $x = 1.27$, where the ratio $N_{Si\text{-}Si}/N_{Si\text{-}N}$ has fallen below 0.02, whereas we have found that this opening occurs in our series at $x \cong 1.1$, where, according to Fig. 9, $N_{Si\text{-}Si}/N_{Si\text{-}N} \cong 0.1$. Two possible causes of this difference can be recognized immediately: First, the use of different criteria to determine the optical gap from the ϵ_2 versus $h\nu$ curves; in this respect, it is worth comparing Fig. 7 of Martín-Moreno *et al.*[7] and Fig. 1 of Dias da Silva *et al.*[8] Second, the presence in our films of substantial amounts of Si—Si, Si—H, N—H, and possibly, N—N bonds for x near the stoichiometric value.

The knowledge of all the atom and bond densities allows us to analyze the kind and mean number of nearest neighbors of each atom; for example, the mean number of N atoms that are nearest neighbors of a Si atom can be calculated as

$$n_N(\mathrm{Si}) = \frac{N_{Si\text{-}N}}{N_{Si}} . \tag{9}$$

These coordination numbers, which can be defined for any type of nearest neighbor, are very useful to analyze the local arrangement around Si and N atoms. Figure 10 shows all types of coordination numbers at Si and N sites as a function of the N concentration. For $x < 1$, N is almost fully coordinated by three Si atoms. At a Si site the number of N nearest neighbors increases linearly with x, with a corresponding decrease of the Si—Si coordination; the Si—H coordination changes from 0.24 in a-Si:H to ~ 0.5 when N is incorporated. Beyond $x \sim 1$ the Si—N coordination at N sites decreases, and H and N atoms may appear as nearest neighbors of N. A similar loss of Si—N coordination at N sites has been reported by Kärcher *et al.*[3] and Misawa *et al.*[2] The flattening of the $n_{Si}(\mathrm{Si})$ curve suggests that this coordination number saturates at approximately 0.5; since $n_H(\mathrm{Si})$ vanishes at high x, this implies that $n_N(\mathrm{Si})$ also saturates at approximately 3.5. No saturation effect is apparent at N sites; nitrogenation over $x = 1.5$ is likely to produce further decrease of $n_{Si}(\mathrm{N})$ and increase of $n_H(\mathrm{N})$ and $n_N(\mathrm{N})$.

At stoichiometric N concentrations, all the bonds other than Si—N are expected to introduce either gap states or resonances in the valence or conduction bands. It is our result that Si—Si bonds may persist up to very high N contents, Si—H bonds tend to disappear, leaving a place for N—H bonds, and N—N bonds may occur for $x > 1$. In addition, the densities of these wrong bonds are found to be substantially larger than those of dangling bonds.

C. Core levels

We have seen in Sec. III that the incorporation of N produces a significant shift of the Si $2p$ peak and an asymmetric broadening. The peak shift is due to the replace-

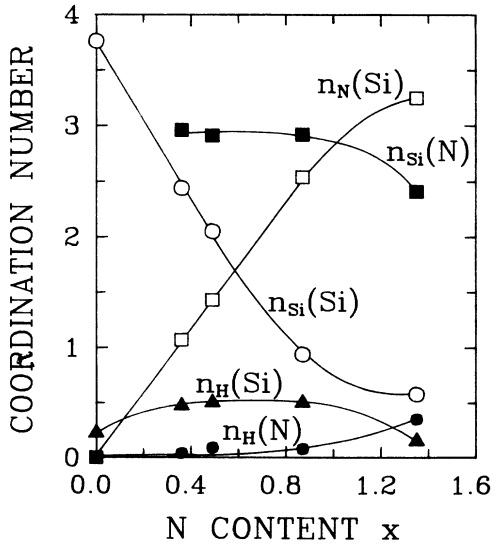

FIG. 10. Coordination numbers at Si and N sites as a function of the N content x. For the definition of these coordination numbers, see Eq. (10).

ment of homopolar Si—Si bonds by heteropolar Si—N bonds; each Si—N bond removes charge from the Si atom, thereby producing an increase in the binding energy of the Si 2p level. If the charge transfer per Si—N bond is independent of the number of N atoms bound to the Si atom, then the mean binding energy must be proportional to the mean number of N atoms bound to a Si atom,

$$\langle E_B(\text{Si } 2p)\rangle = E_B^0 + \Delta E_{\text{Si—N}}\, n_{\text{N}}(\text{Si}) , \quad (10)$$

where E_B^0 is the binding energy of Si 2p in a-Si:H and $\Delta E_{\text{Si—N}}$ is the chemical shift per Si—N bond.[24] Figure 11 shows the mean binding energy, evaluated with the fitting discussed in Sec. III, as a function of $n_{\text{N}}(\text{Si})$. Assuming a linear relationship, we obtain $\Delta E_{\text{Si—N}} = 0.78$ eV, in excellent agreement with the values derived by Kärcher *et al.*[3] decomposing the Si 2p spectrum into five components.[25] Inverting Eq. (10), we obtain $n_{\text{N}}(\text{Si}) = 2.95$ for sample 5, which falls well in the corresponding curve in Fig. 10. If we convert the binding-energy shift into charge transfer using the scale factor deduced by Grunthaner *et al.*,[26] 2.2 eV/electron, we obtain a charge transfer of 0.35e per Si—N bond; this value is in between the $\cong 0.1e$ deduced from calculations by Martín Moreno *et al.*[7] and the $\cong 0.6e$ and 0.73e obtained by Ferreira and Gonçalves da Silva[6] and Ren and Ching,[4] respectively. Thus, calculations fail in predicting an ionicity either too low or too high.

The Si 2p line shape is determined by the distribution $f(k)$ of Si atoms with $k = 0$, 1, 2, 3, or 4 Si—N bonds. All the Si atoms with k Si—N bonds contribute to a region of the Si 2p spectrum at an energy $k\,\Delta E_{\text{Si—N}}$ from the peak in a-Si:H. At low N concentrations (sample 2) the positive asymmetry indicates a predominance of Si atoms with none or one Si—N bond; the Si atoms with two, three, and four Si—N bonds produce the tail towards high binding energies. At an intermediate N concentration (sample 3) the peak is more symmetric, indicating that Si atoms with two Si—N bonds dominate; the high probability of finding Si atoms with fewer or more Si—N bonds makes the peak broader than at $x = 0$ and 1.35. At higher N contents (sample 4) the negative asymmetry indicates that the majority of the Si atoms have three or four Si—N bonds, the tail towards low binding energies being produced by the Si atoms with fewer Si—N bonds. Finally, in the most nitrogenated sample each Si atom is surrounded by as many N atoms as possible, and the Si 2p peak becomes narrower and more symmetric.

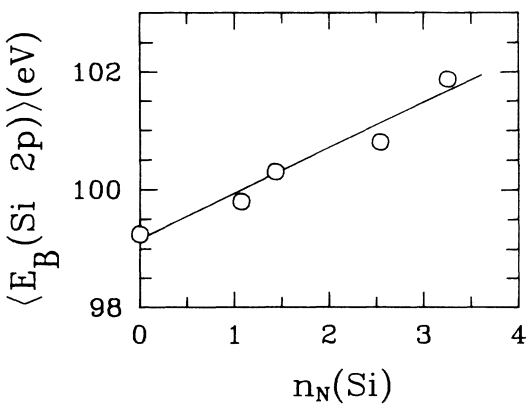

FIG. 11. Mean binding energy of the Si 2p peak plotted against the mean number of N atoms bound to a Si atom.

The position and line shape of the N 1s peak is also determined by the kind and distribution of the nearest neighbors of the N atoms. For $x < 1$ the peak position is practically constant, in agreement with the almost complete coordination of N with Si atoms deduced in the preceding subsection. For the most nitrogenated sample, we have found that some Si—N bonds are replaced by the less ionic N—H and, possibly, N—N bonds. This change of nearest neighbors reduces the negative charge on the N atoms, producing the 0.4-eV increase in the binding energy of the N 1s level. This N 1s chemical shift, evidenced by referring the energies to the Ar $2p_{3/2}$ level, has been ignored in the work of Kärcher *et al.*;[3] consequently, their plot of the band edges and ε_F as a function of x, made by considering the N 1s level as a "constant" reference level, must be partially incorrect. We associate the slight broadening of the N 1s peak with a second-coordination-shell effect. As the N concentration increases, N atoms appear as second neighbors of N; the different arrangements produce small unresolved shifts which result in a broadening of the peak.

V. SUMMARY

We have measured electron-energy-loss and x-ray photoelectron spectra from a-SiN_x:H in the range $0 \le x < 1.5$. By combining the results of EELS and quantitative XPS with measurements of ir absorption, we have been able to determine all the atom and bond densities. In addition, the analysis of the (XPS) peak shifts and line shapes, which are not involved in the derivation of the densities, serves to confirm results and/or yield more information.

In particular, we have found the following.

(i) There is no segregation of nonstoichiometric films into amorphous silicon and stoichiometric silicon nitride.

(ii) There is a linear relationship between the density of Si—N bonds and the integrated absorption $I_{\text{Si—N}}$; the proportionality constant is $A_{\text{Si—N}} = 1.76 \times 10^{19}$ cm^{-2}.

(iii) For $x < 1$ the most important change is the replacement of Si—Si bonds by Si—N bonds; N atoms are almost fully coordinated by three Si atoms; Si atoms have N, H, and other Si atoms as nearest neighbors.

(iv) For $x > 1$, Si—Si and Si—H bonds are replaced by Si—N bonds; this is, however, not enough to saturate the three N valencies with Si, and some N—H and, possibly, N—N bonds appear.

(v) At stoichiometric concentrations there is a substantial amount of Si—Si and N—H bonds.

(vi) The opening of the optical gap occurs when the ratio $N_{\text{Si-Si}}/N_{\text{Si-N}}$ falls below 0.10.

(vii) Only three electrons per N atom participate in the plasma oscillations; the calculated mass densities of a-Si:H and a-$SiN_{1.35}$:H are very near the densities of the crystalline forms, thereby indicating that the plasmons

penetrate only slightly into the voids of the amorphous network.

(viii) The Si $2p$ chemical shift increases linearly with the mean number of N-atom nearest neighbors of Si. The chemical shift per Si—N bond is 0.78 eV, which means a charge transfer of $0.35e$.

ACKNOWLEDGMENTS

We thank for their expert technical assistance J. De Pellegrin and C. Wenger. One of us (H.A.) acknowledges partial support by Consejo Nacional de Investigaciones Cientificas y Técnicas (CONICET), Argentina.

[1]T. Aiyama, T. Fukunaga, K. Niihara, T. Hirai, and K. Suzuki, J. Non-Cryst. Solids **33**, 131 (1979).

[2]M. Misawa, T. Fukunaga, K. Niihara, T. Hirai, and K. Suzuki, J. Non-Cryst. Solids **34**, 313 (1979).

[3]R. Kärcher, L. Ley, and R. L. Johnson, Phys. Rev. B **30**, 1896 (1984).

[4]S. -Y. Ren and W. Y. Ching, Phys. Rev. B **23**, 5454 (1981).

[5]J. Robertson, Philos, Mag. B **44**, 215 (1981); J. Appl. Phys. **54**, 4490 (1983); J. Robertson and M. J. Powell, Appl. Phys. Lett. **44**, 415 (1984).

[6]E. C. Ferreira and C. E. T. Gonçalves da Silva, Phys. Rev. B **32**, 8332 (1985).

[7]L. M. Martín-Moreno, E. Martinez, J. A. Vergés, and F. Yndurain, Phys. Rev. B **35**, 9683 (1987).

[8]J. H. Dias da Silva, J. I. Cisneros, F. C. Marques, and M. P. Cantão, in *Current Topics of Semiconductor Physics,* edited by O. Hipolito, A. Fazzio, and G. E. Marques (World Scientific, Singapore, 1988); J. I. Cisneros, J. H. Dias da Silva, M. P. Cantão, and F. C. Marques, Thin Solid Films (to be published).

[9]Ar atoms were implanted in the samples during the preparation and/or the cleaning process.

[10]The absence of the Si—O vibrational band in the ir spectra indicates that the O concentration in the bulk material was smaller than 1 at. %.

[11]Sample 5 was part of a series prepared for a different study; only the optical gap and XPS measurements were performed, and they are presented in Tables I and II.

[12]J. Tauc, in *Optical Properties of Solids,* edited by F. Abelès (North-Holland, Amsterdam, 1972), Chap. 5.

[13]H. Kurata, M. Hirose, and Y. Osaka, Jpn. J. Appl. Phys. **20**, L811 (1981).

[14]M. H. Brodsky, M. Cardona, and J. I. Cuomo, Phys. Rev. B **16**, 3556 (1977).

[15]H. Shanks, C. J. Fang, L. Ley, M. Cardona, F. J. Demond, and S. Kalbitzer, Phys. Status Solidi **100**, 43 (1980).

[16]A. Morimoto, Y. Tsujimura, M. Kumeda, and T. Shimizu, Jpn. J. Appl. Phys. **24**, 1394 (1985).

[17]H. R. Philipp, J. Electrochem. Soc. **120**, 295 (1973); C. Chaussat, E. Bustarret, and A. Deneuville, J. Non-Cryst. Solids **77-78**, 917 (1985).

[18]H. Raether, in *Excitation of Plasmons and Interband Transitions by Electrons,* edited by G. Höhler (Springer, Berlin, 1980).

[19]L. Ley, in *The Physics of Amorphous Silicon,* edited by J. D. Joannopoulos and G. Lucovsky (Springer, Heidelberg, 1984).

[20]In these spectra we have referred the energies to the Fermi level of a Ag sample. To this end we recorded Ag $3d_{5/2}$ spectra before and after each valence-band spectrum.

[21]D. Hardie and K. H. Jack, Nature (London) **180**, 332 (1957).

[22]T. Makino, J. Electrochem. Soc. **130**, 450 (1983).

[23]G. Sasaki, M. Kondo, S. Fujita, and A. Sasaki, Jpn. J. Appl. Phys. **21**, 1394 (1982); C. Chaussat, E. Bustarret, J. C. Bruyere, and R. Groleau, Physica **129B**, 215 (1985).

[24]The presence of H can be taken into account by including a term $\Delta E_{\mathrm{Si-H}}\, n_{\mathrm{H}}(\mathrm{Si})$. However, its contribution is negligible since $n_{\mathrm{H}} \leq 0.52$ and $\Delta E_{\mathrm{Si-H}} = 0.33$ eV [L. Ley, J. Reichardt, and R. L. Johnson, Phys. Rev. Lett. **49**, 1664 (1982)].

[25]We point out that our procedure does not require the decomposition of the Si $2p$ spectrum into its components; our fitting with up to five Gaussians has been used only to evaluate the mean binding energy, and any other kind of fitting is equally good for this purpose.

[26]F. J. Grunthaner, P. J. Grunthaner, R. P. Vasquez, B.F. Lewis, J. Maserjian, and A. Madhukar, Phys. Rev. Lett. **43**, 1683 (1979).